# Dynamic Light Scattering from Block Copolymer Melts near the Order−Disorder Transition

**P. Stepanek**

*Institute of Macromolecular Chemistry, Czech Academy of Sciences, Prague, Czech Republic*

**T. P. Lodge***

*Department of Chemistry, University of Minnesota, Minneapolis, Minnesota 55455-0431*

*Received July 10, 1995; Revised Manuscript Received December 4, 1995*[⊗]

ABSTRACT: Dynamic light scattering measurements have been performed on four symmetric diblock copolymer melts, as a function of temperature, both above and below the order−disorder transition (ODT). The materials were poly(ethylenepropylene)−poly(ethylethylene) (PEP−PEE) with $M_w = 5.0 \times 10^4$, poly(vinylcyclohexane) (PVCH)−PEE with $M_w = 5.3 \times 10^4$, PVCH−polyethylene (PE) with $M_w = 1.6 \times 10^4$, and PE−PEE with $M_w = 2.7 \times 10^4$. Up to four relaxation modes were resolved. In all cases, the correlation functions exhibited a very strong, very slow diffusive mode, similar to that previously observed in polymeric and small-molecule glass formers and attributed to long-range density fluctuations. Via the Kawasaki−Stokes−Einstein relation, a correlation length or cluster size, $\xi$, was associated with this process. Above the ODT, $\xi$ was on the order of 100 nm and independent of temperature. However, below the ODT, $\xi$ apparently increased by at least 2 orders of magnitude for PVCH−PE and PE−PEE, while remaining nearly independent of temperature for the other two copolymers. For PEP−PEE, the angle dependence of the scattered intensity also reflected a correlation length of 100 nm. The cluster mode was subtracted from the correlation functions, and the residual decays were reanalyzed by Laplace inversion. Two other modes, the diffusive heterogeneity mode and the structural internal mode, were then resolved, in accordance with theory. For the PEP−PEE sample, the heterogeneity diffusion coefficient was in quantitative agreement with the self-diffusion coefficient as measured by forced Rayleigh scattering, and at least in the disordered state, the relaxation time of the internal mode was in quantitative agreement with the longest relaxation time determined by rheological measurements. For this sample, a fourth, diffusive mode was also apparent, with a time scale intermediate between the longest relaxation time and the translational diffusion of the chains. The temperature dependence of this mode was weaker than that of the viscosity or the chain diffusion, and its specific origin is unclear; however, it appears to be correlated with the frequency at which time−temperature superposition breaks down in the rheological properties.

## Introduction

Diblock copolymers consist of two covalently bonded sequences of monomers A and B. In a melt, AB copolymers may be disordered or they may self-assemble into various microstructures, depending on temperature $T$, on the magnitude of the interaction parameter $\chi$ between A and B, and on the architecture of the copolymer: the total degree of polymerization, $N$, and the composition $f$ (fraction of A monomers). Such materials have very interesting practical applications, and in recent years they have become the focus of extensive investigation.[1]

The phase diagram for diblock copolymers has been described by Leibler in the framework of a mean-field theory,[2] subsequently extended to include fluctuation effects.[3−5] For a given composition, the product $\chi N$ determines the equilibrium state of the copolymer. At high temperature, $\chi N \ll 10$, and the copolymer melt is disordered; A and B segments are homogeneously mixed. With decreasing temperature, an order−disorder transition (ODT) appears, located for a symmetric diblock ($f = 0.5$) at $\chi N_{ODT} \approx 10.5$ in the mean-field theory and at $\chi N_{ODT} \approx 10.5 + 41/\bar{N}^{-1/3}$ in the fluctuation theory ($\bar{N} \equiv Na^6v^{-2}$, where $a$ is the statistical segment length and $v$ the segment volume). For disordered samples with $\chi N \approx 10$, substantial composition fluctuations have been observed.[6,7] For $\chi N \gg 10$ the melt adopts one of several possible ordered morphologies; examples include lamellar, cylindrical, spherical, and bicontinuous cubic structures.[1,8,9]

The collective dynamics of block copolymer melts have been studied by rheology,[6,10] which is sensitive both to the ODT and to the composition fluctuations near the transition. Potential limitations to the rheological approach are a limited frequency window at a given temperature and the possibility of perturbing the system under study, particularly for weakly ordered materials. Dynamic light scattering (DLS) is a noninvasive technique with a wide dynamic range (at least $10^{-6}$−$10^3$ s) that could be applicable. However, rather few papers have been published dealing with polarized light scattering from block copolymer melts;[11−13] this may reflect, in part, experimental difficulties related to the preparation of dust-free melt samples, and to the presence of unexpectedly intense scattering in such materials, as will be described herein.

Heretofore, three copolymers have been investigated by polarized DLS: poly(ethylene-*b*-ethylethylene),[11] poly(styrene-*b*-methylphenylsiloxane),[12] and poly(ethylmethylsiloxane-*b*-dimethylsiloxane).[13] Additional materials have been investigated by depolarized DLS, which is more sensitive to local segmental dynamics.[14] DLS from block copolymers has recently been reviewed.[15] In the present paper, we have extended our previous report[11] to include four chemically different block copolymers and to present a comparison of light scattering results with those obtained by forced Rayleigh scattering[16,17] and rheology.[10] In the next section, we review the relaxation modes expected on the basis

[⊗] Abstract published in *Advance ACS Abstracts,* February 1, 1996.

0024-9297/96/2229-1244$12.00/0 

of theory. Following a description of the experimental procedures, we then present the results. A major, unanticipated feature is the consistent appearance of a large-amplitude, very slow diffusive mode. It bears a strong resemblance to the slow mode explored in polymeric and nonpolymeric glass formers by Fischer and co-workers, and which was ascribed to long-range density fluctuations.[18] Other modes are also resolved and analyzed in the context of available theory.

## Theoretical Background

The current description of the dynamic structure factor of disordered block copolymer liquids (melts and solutions) is founded on two complementary theoretical approaches. The first, due to Benmouna *et al.*,[19,20] follows the linear response formalism for multicomponent systems of Akcasu *et al.*[21,22] and utilizes a dynamical mean-field (random-phase) approximation. For block copolymers in nonselective good solvents, two dynamic modes are predicted: a cooperative diffusion mode, reflecting relaxation of fluctuations in total polymer concentration (as also observed in homopolymer solutions), and an internal chain mode arising from the relative motions of the two blocks. The latter mode has a decay rate, $\Gamma$, independent of wavevector, $q$, whenever $qR_g \ll 1$, where $R_g$ is the radius of gyration of the coil. The second theory, of Semenov *et al.*,[23,24] takes into account the fact that all real copolymers exhibit some heterogeneity in composition, *i.e.*, fluctuations in $f$ from chain to chain. This permits fluctuations in relative block concentration of arbitrarily long wavelength (*i.e.*, $q \rightarrow 0$) and generates an additional diffusive DLS mode, with decay rate governed by the translational diffusion of the whole chains. We refer to this as the "heterogeneity" mode to emphasize that it reflects variations in chemical composition, rather than in molecular weight; however, the terminology "polydispersity mode" has also been employed.[24,25] This mode is analogous to that described by Pusey *et al.*[26] for mixtures of hard spheres which differ in optical scattering power. All three modes (cooperative, internal, and heterogeneity) have been well-documented experimentally for polystyrene−polyisoprene diblocks of various molecular weights, in dilute and semidilute solutions, and in various solvents.[24,25,27,28]

For a block copolymer melt the cooperative diffusion is not present, and the expected dynamic structure factor can thus be written

$$\frac{S(q,t)}{S(q,0)} = A_I \exp(-\Gamma_I t) + A_H \exp(-\Gamma_H t) \qquad (1)$$

where the subscripts I and H denote the internal and heterogeneity modes, respectively. This relation assumes that the two modes are uncoupled. In a melt of identical copolymer chains, a fluctuation in composition can only be created on length scales of $\leq R_g$, by relative motion of the centers of mass of block A and block B. The corresponding relaxation process is characterized by a decay rate $\Gamma_I$ which, for $qR_g \ll 1$ and to within a constant of order unity, is equal to $\tau_1^{-1}$, where $\tau_1$ is the longest viscoelastic relaxation time of the chain. For low molecular weights, $\tau_1$ is the Rouse time:

$$\tau_1 = \tau_o N^2 \qquad (2)$$

where $\tau_o$ is the characteristic microscopic time for one segment and $N$ is the number of segments in the chain. On the other hand, in the entanglement regime the reptation model predicts that $\tau_1$ is increased by a factor of $N/N_e$ over the Rouse result, where $N_e$ is the number of segments between entanglements. Experimentally, the data may be better represented by $\tau_1 \sim N^{3.4}$; furthermore, in the presence of substantial fluctuations, chain relaxation can be retarded by an additional factor.[29] The amplitude of the internal mode is given by[23,24]

$$A_I \propto (n_A^2 - n_B^2)^2 f^2 (1-f)^2 N (qR_g)^2 \qquad (3)$$

where $n_A$ and $n_B$ are the refractive indexes of the blocks.

The heterogeneity mode is characterized by a decay rate[23,24]

$$\Gamma_H = q^2 D_H = q^2 D(1 - 2\kappa\chi N) \qquad (4)$$

where $D$ represents the diffusion coefficient of the chains (assumed to be insensitive to small variations in composition) and $\kappa$ is the heterogeneity factor defined below.[23,24] The amplitude of this mode is then predicted to be

$$A_H \propto (n_A^2 - n_B^2)^2 \frac{\kappa N}{1 - 2\kappa\chi N} \qquad (5)$$

The heterogeneity mode is sensitive to the degree of variation in composition from chain to chain, which is expected to be small for anionically polymerized, narrow molecular weight distribution samples. Under the assumption that the molecular weight polydispersities of the two blocks are statistically independent

$$\kappa \cong 2\delta \frac{f^2(1-f)^2}{f^2 + (1-f)^2} \qquad (6)$$

where $\delta = (M_w/M_n) - 1$.[23,24] For symmetric copolymers with $M_w/M_n < 1.1$, $\kappa < 0.025$. Comparing eqs 3 and 5, $A_H$ should be greater than $A_I$ for most narrow distribution samples.

## Experimental Section

**Samples.** In the present work we have used four anionically synthesized symmetric block copolymers kindly provided by Bates and co-workers;[7,30,31] they are listed, together with their main characteristics, in Table 1. The chemical constituents are poly(ethylenepropylene) (PEP), poly(ethylethylene) (PEE), poly(vinylcyclohexane) (PVCH), and polyethylene (PE), in various combinations; the prefix d indicates deuteration.

**Table 1. Sample Characteristics**

| sample | $T_{ODT}$, °C | $M_w \times 10^4$ | $f_A$ |
|---|---|---|---|
| PEP−PEE-2 | 96 | $5.0_1$ | 0.55 |
| PVCH−PEE-2 | 229 | 5.3 | 0.48 |
| PVCH−dPE-1 | 235 | 1.6 | 0.48 |
| PE−PEE-8 | 136 | $2.7_5$ | 0.50 |

In order to prepare optically clean samples, the block copolymers were dissolved in pentane or hexane at a concentration of 0.05 g/mL and filtered through a G5 filter (Jena, Germany) into de-dusted light scattering cells. The majority of the solvent was then slowly evaporated through a membrane in an oven at 50 °C. The cells were then linked to a vacuum line, where the remainder of the solvent was evaporated and the cells were sealed.

**Measurements.** The DLS instrument consists of a homemade goniometer with a Hamamatsu R869 photomultiplier and an $Ar^+$ laser (Coherent Innova-70). The photomultiplier output is linked to an ALV-5000 correlator operating with 288 channels, covering ~11 decades of delay time. Since a wide

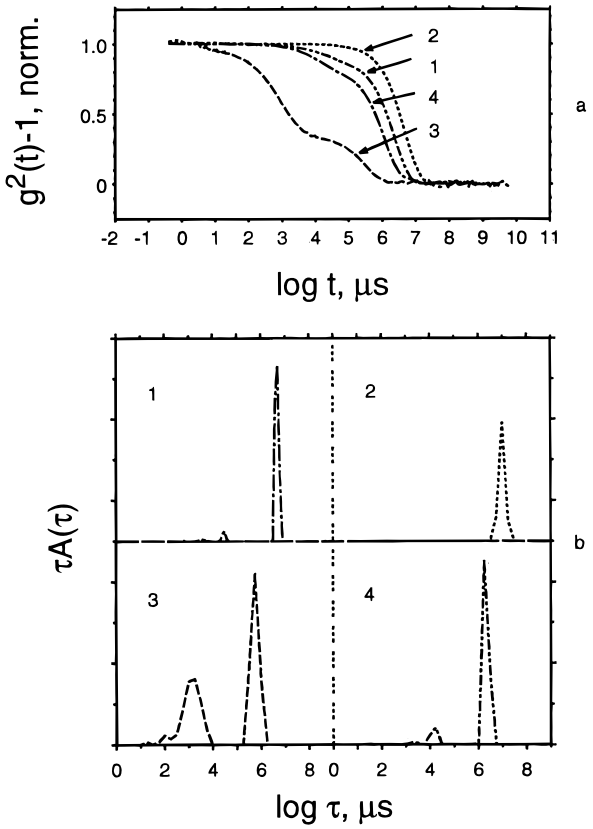


**Figure 1.** (a) Normalized intensity correlation functions for $\theta = 90°$ and (b) corresponding distributions of decay times for (1) PEP−PEE-2 at 202 °C, (2) PE−PEE-8 at 180 °C, (3) PVCH−dPE-1 at 270 °C, and (4) PVCH−PEE-2 at 270 °C.

distribution, $A(\tau)$, of decay times, $\tau$, is expected, the correlation functions were analyzed with the program REPES,[32−34] which targets the inverse Laplace transformation:

$$g^{(1)}(t) = \int A(\tau) \exp(-t/\tau)\, d\tau \qquad (7)$$

where $g^{(1)}(t)$ is the field correlation function. The program REPES is similar to the widely used program CONTIN,[35] except that REPES actually inverts the measured intensity correlation function $g^{(2)}(t) = 1 + \gamma|g^{(1)}(t)|^2$, where $\gamma$ is an instrumental constant.

## Results and Discussion

**Cluster Mode.** Figure 1a shows representative normalized intensity correlation functions $g^{(2)}(t)$ for each polymer, obtained at a scattering angle of 90° and at the temperatures indicated. The most noticeable feature is the presence of a very slow decay in all the samples, which dominates the correlation function for all but the PVCH−PE sample. Distribution functions $A(\tau)$ have been extracted from $g^{(2)}(t)$, using the inverse Laplace transformation, and they are shown in Figure 1b in the equal area representation ($\tau A(\tau)$ vs log $\tau$). The slow mode has a typical decay time of 1 s or longer, at the temperatures indicated, and the width of the peak is narrow. The additional, lower amplitude features, with decay times in the range 1−100 ms, will be discussed subsequently.

Figure 2 demonstrates that the slow mode is diffusive, since the decay rate exhibits a linear dependence on $q^2$ and passes through the origin. Although data from only two samples are illustrated in the figure, this diffusive character has been established for all four block copolymer materials used in this work. It is thus possible to assign a "cluster" diffusion coefficient, $D_{cl}$, to this

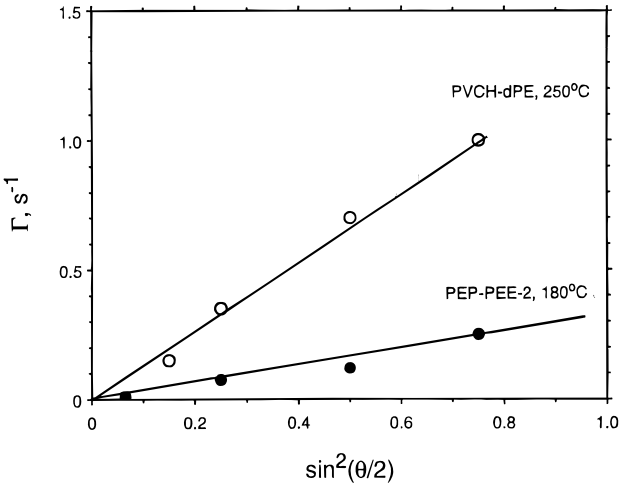


**Figure 2.** Angle dependence of the decay rate of the cluster mode.

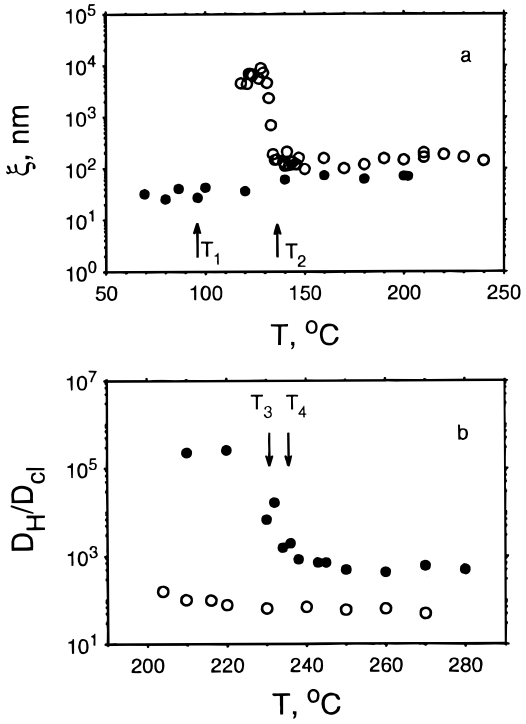


**Figure 3.** Temperature dependence of the hydrodynamic size corresponding to the cluster mode: (a) $\xi$ for PEP−PEE-2 (●), ODT at $T_1$, and PE−PEE-8 (○), ODT at $T_2$; (b) $D_H/D_{cl}$ for PVCH−PEE-2 (○), ODT at $T_3$, and PVCH−dPE-1 (●), ODT at $T_4$.

process. It is also possible, using known values of the shear viscosity, $\eta$, to determine a hydrodynamic size or correlation length, $\xi$, corresponding to this very slow diffusion process, through the Kawasaki−Stokes−Einstein equation,

$$\xi = kT/6\pi\eta D_{cl} \qquad (8)$$

Figure 3a displays the temperature dependence of $\xi$ obtained in this way for PEP−PEE-2 and PE−PEE-8. For PEP−PEE-2, $\xi$ is approximately constant at 60 nm in the disordered phase, down to $T_{ODT} = 96$ °C. The observed slight decrease in $\xi$ below $T_{ODT}$ may not be real, since the value of $\eta$ used in eq 8 was based on WLF extrapolation from the disordered state. For PE−PEE-8, also, $\xi$ is approximately constant in the disordered phase above $T_{ODT} = 136$ °C, and of similar magnitude:

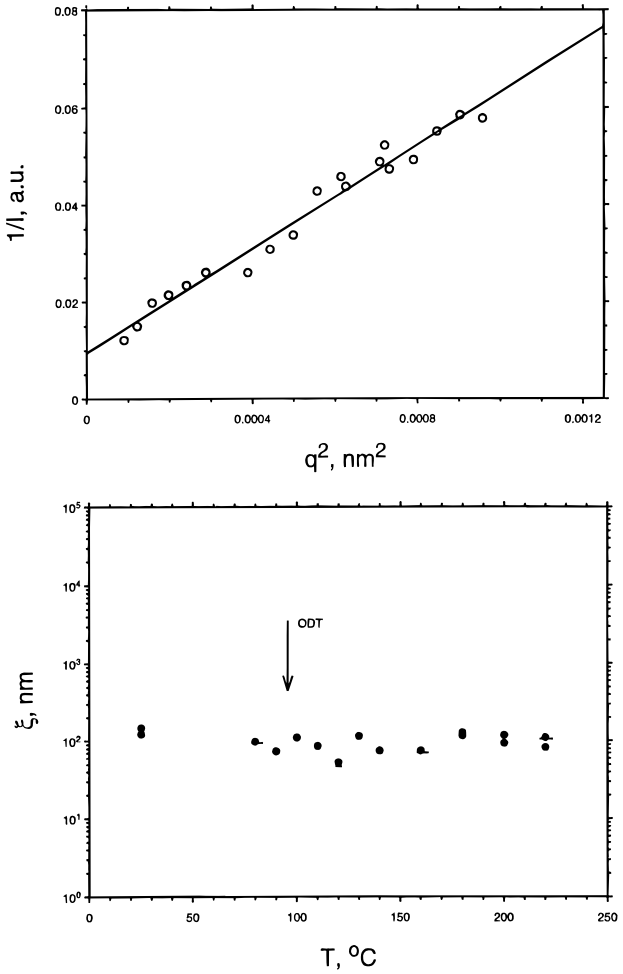


**Figure 4.** Static light scattering from PEP−PEE-2: (a, top) inverse intensity as a function of $q^2$ at 160 °C and (b, bottom) the resulting correlation length as a function of temperature.

$\xi \approx 100$ nm. The difference between PE−PEE-8 and PEP−PEE-2 is that for the former there is a substantial decrease in $D_{cl}$ just below the ODT.

Similar phenomena have been observed for the other two block copolymers examined, PVCH−PE and PVCH−PEE. $\eta$ values were not available for these two materials, since at temperatures above $T_{ODT}$ they were outside the range of the rheometer; nevertheless, some information on the cluster mode can be obtained. We shall demonstrate below that one of the faster components of $A(\tau)$ corresponds to the heterogeneity diffusion coefficient, $D_H$, that $D_H$ is insensitive to the ODT, and that its dependence on temperature is governed only by that of the viscosity. Thus, from the ratio $D_H/D_{cl}$ we can obtain an estimate of the temperature dependence of $\xi$. Figure 3b displays the temperature dependence of $D_H/D_{cl}$ for the copolymers PVCH−PEE and PVCH−PE. For the latter copolymer, $\xi$ increases near $T_{ODT}$ by at least 2 orders of magnitude, whereas for the former, $\xi$ is practically constant with temperature through the ODT.

Although there is as yet no rigorous justification for the application of eq 8 to this problem, it provides a useful means to associate an approximate length scale with the observed dynamic phenomenon. Furthermore, the same correlation length may be inferred from the angle dependence of the scattered intensity, which is completely independent of eq 8. For example, in Figure 4a we present the inverse scattered intensity vs $q^2$ for PEP−PEE-2 at 160 °C. A reasonably linear plot results, with $\xi \approx 75$ nm. In Figure 4b, $\xi$ thus obtained is plotted as a function of temperature. Within the scatter, a constant value of ∼100 nm is determined. The data points with bars were taken after overnight annealing at the selected temperature. One may conclude that, at least over this time scale, the results are independent of time.

As a working hypothesis, we attribute the cluster mode to the same long-range density correlations observed in other homopolymer and block copolymer melts and low molecular weight glass formers.[12,13,18] If this is indeed the case, then the phenomenon is unrelated to the block copolymer nature of the chains. In support of this picture is the observation of a similar mode in a PE homopolymer melt; interestingly, no such mode was apparent in a PEP homopolymer melt.[36] This would imply that a PEE homopolymer melt should exhibit a cluster mode, in order to account for its presence in PEP−PEE-2.

There remains the interesting observation that, for two of the copolymers, the cluster mode undergoes an abrupt slowing down near the ODT, whereas for the other two, it does not. To what property of the chains does this slowing down correlate? It is present for the two lower molecular weight chains, both of which contain PE. However, it is not an entanglement effect, as PEP−PEE-2 is more entangled, and PVCH−PEE-2 less entangled, than the other samples. Nor is it correlated with the distance from $T_{ODT}$ to $T_g$ or $T_m$; only for PE−PEE-8 is $T_{ODT}$ much within 100 °C of $T_m$ (108 °C for PE; $T_g$ is ∼137 °C for PVCH, −20 °C for PEE, and −56 °C for PEP).[30,31] In the fluctuation picture of block copolymers, the ODT should be more strongly first order for lower molecular weight chains, which is qualitatively consistent with the observations in Figure 3. Thus we are led to speculate that the slowing down of the cluster mode in the PE-containing copolymers is due to the abrupt increase in the spatial coherence of the microdomains (*i.e.*, regions rich in PE segments) at the ODT. Note that, above the ODT, the composition fluctuations correspond to local regions similarly rich in PE segments, but they do not have spatial correlations on the length scale corresponding to the apparent cluster size.

**Subtraction Technique.** The presence of the cluster mode is a major obstacle to a detailed analysis of the intermediate region of the correlation function. The large amplitude of this mode inhibits a reliable determination of the other, weaker components of the spectrum of decay times, which sometimes have a combined amplitude amounting to less than 5% of the total. Furthermore, as the strong component has a very narrow distribution (effectively a single-exponential decay, *vide infra*), it can generate spurious peaks in the remaining part of the spectrum of decay times, via the so-called $\delta$ effect.[37] To overcome this difficulty, we consistently used the subtraction technique,[38] wherein a calculated correlation function corresponding to the cluster mode was subtracted from the measured correlation function, including any possible baseline term, and the remainder, representing the fast and intermediate parts of the original correlation function, was reanalyzed using REPES. A more detailed description of this approach has been given.[38] Using simulated data with the same delay time structure as in the experiments, and with a noise level corresponding to a typical measurement, we have ascertained that this subtraction procedure yields the correct decay times. The simulations were performed for cases where one or two closely

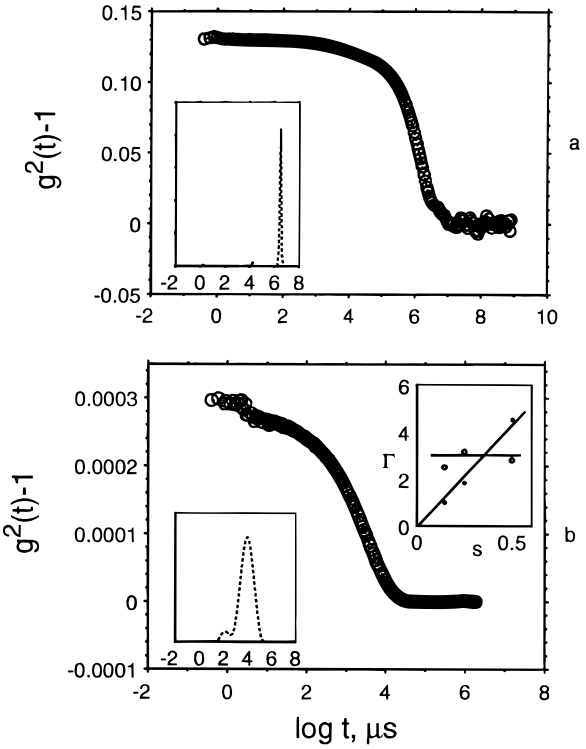


**Figure 5.** (a) Full correlation function and distribution of decay times (inset) for PEP−PEE-2 at 220 °C; (b) after subtraction of cluster mode. The inset in the upper right corresponds to the decay rate (in kHz) vs $s = \sin^2(\theta/2)$ for faster (○) and slower (●) modes.

spaced weak components were added to a strong $\delta$ function located at large delay times.

**Heterogeneity Mode.** Figure 5 illustrates this procedure with (a) the original correlation function and (b) the subtracted one, obtained on PEP−PEE-2 at 220 °C; the corresponding spectra of decay times are shown as insets. Two components can be identified in Figure 5b, and the corresponding dependence on scattering angle is also illustrated in an inset. The decay rate of the slower, larger component is linear in $q^2$ and goes through the origin, so that it corresponds to a diffusive process. The data for the angle dependence of the faster, low-amplitude component in Figure 5b are scattered, but are consistent with an angle-independent relationship. Additional support for this conclusion comes from a "global analysis" of the correlation functions; *i.e.*, correlation functions obtained at several angles for a given sample have been analyzed simultaneously by a modified version of the program CONTIN, described in detail elsewhere.[39] For each set of angles, two distributions of decay times have been extracted from the set of correlation functions, one containing all diffusive decays, and the other containing all angle-independent decays. This approach assumes that the angle dependence (if any) of the amplitudes of all modes is identical. Figure 6 shows these results for the data from Figure 5. The left grid displays angle-independent (purely relaxational) components, the right grid the diffusive ones. This procedure thus confirms that the fast mode in Figure 5 has a relaxational character, whereas the slow, dominant one is diffusive. The shoulder located at log $\tau \approx 3.3$ in the diffusion grid on Figure 6 will be discussed later.

The diffusion coefficient extracted from the slower component in Figure 5b is displayed as a function of temperature in Figure 7, together with values of $D_s$, the

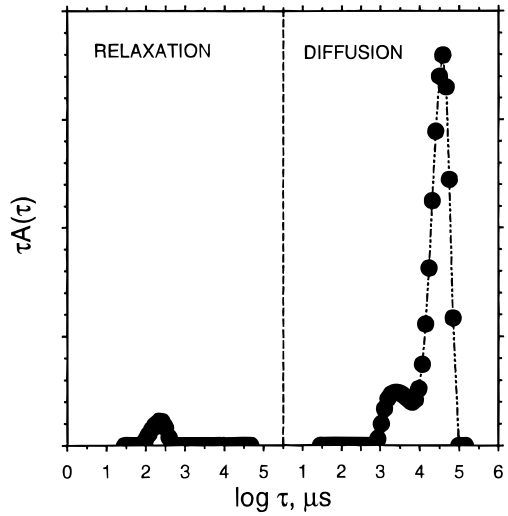


**Figure 6.** Global Laplace inversion results for PEP−PEE-2 at 220 °C using data from $\theta = 45°$, 60°, 90°, and 120°. The distribution function for the diffusive modes corresponds to $\theta = 90°$.

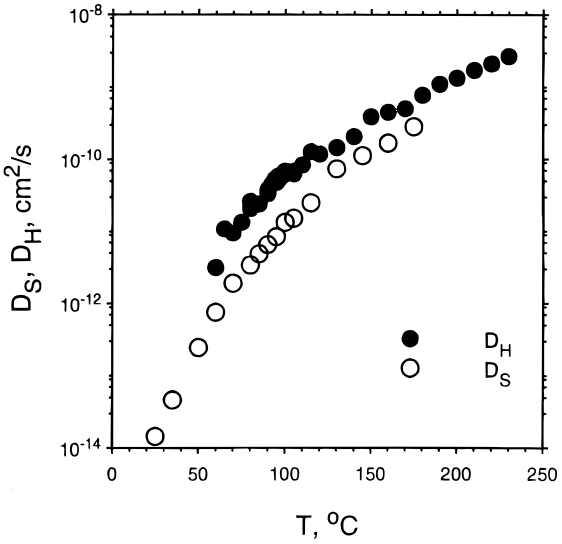


**Figure 7.** Temperature dependence of self-diffusion (forced Rayleigh scattering) and heterogeneity mode diffusion coefficients for PEP−PEE-2.

self-diffusion coefficient, obtained for this copolymer (PEP−PEE-2) by forced Rayleigh scattering.[17,40] The similar values and temperature dependences of the two diffusion coefficients throughout the common temperature range lead us to identify this DLS mode as the heterogeneity mode. However, it is clear that $D_H > D_s$ by a factor of ~5; an explanation for this will be presented later.

**Internal Mode.** Figure 8 demonstrates that the weak fast component seen in Figure 5b and in the relaxation grid of Figure 6 corresponds to the longest internal relaxation time $\tau_1$ of the copolymer chain, as predicted. The smooth curve in Figure 8 represents values of $\tau_1$ calculated from rheological measurements.[10] As $G' \approx G''$ for $\omega\tau_1 = 1$, we have extracted $\tau_1$ from plots of log $G'$ and log $G''$ vs log($\omega a_T$) as the intersection of the straight lines in the (terminal) low-frequency regime; $a_T$ is the shift factor. The smooth curve then represents a fit of these data to the WLF equation. The agreement between values of $\tau_1$ extracted from light scattering and those calculated from rheological measurements is very good above $T_{ODT}$. In the ordered state, however, the experimental points do not follow

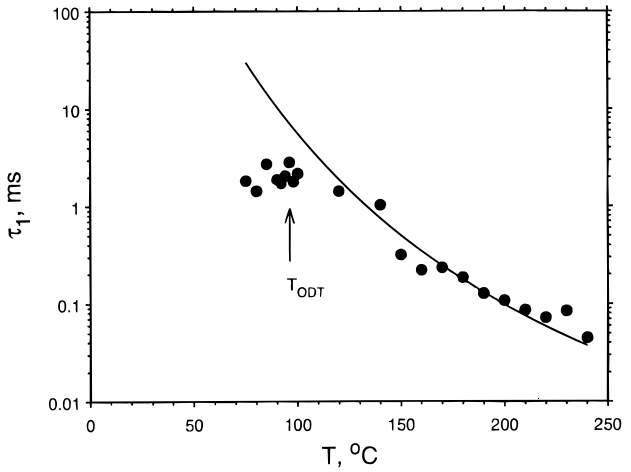


**Figure 8.** Temperature dependence of the relaxation time of the internal mode, compared to the longest relaxation time from rheology (smooth curve), for PEP−PEE-2.

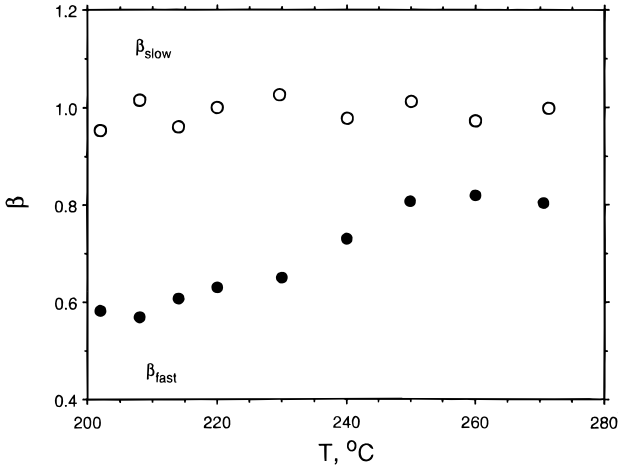


**Figure 9.** Temperature dependence of the stretched-exponential exponents, $\beta$, for the cluster (slow) and fast modes for PVCH−PEE-2.

the curve. One should note first that the latter is an extrapolation of the rheological data into the ordered phase and is therefore not necessarily a reliable measure of $\tau_1$ for $T < T_{ODT}$. Second, the light scattering relaxation time exhibits a *weaker* temperature dependence than the segmental dynamics reflected in the WLF equation. This observation suggests that it no longer corresponds to relaxation of the chain end-to-end vector but rather to composition fluctuations on a more local scale.

A remark needs to be made about the global analysis technique discussed above. We have shown that, at least in the disordered state, the relaxational component on the left grid of Figure 6 corresponds to the first internal mode of the copolymer chain. However, eq 3 predicts that $A_I$ depends linearly on $q^2$, whereas the global analysis assumes that it is angle independent. The relative amplitude of this component is very weak (typically only 4% even after subtraction), and simulations have shown that in such a case the presence of a relaxational component with an average amplitude is better than no relaxational component at all and that it has approximately the correct decay time.

**Intermediate Mode.** Close examination of the peak corresponding to the heterogeneity mode on all the systems investigated reveals that its width is greater than would be expected for a single process, and for the copolymers containing PVCH it is particularly noticeable that the width increases with decreasing temperature. Since the width of a peak obtained by Laplace inversion is not a particularly reliable quantity (for example, it is quite sensitive to the degree of regularization), we have instead fitted the (unsubtracted) correlation functions for this system to a double Williams−Watt function:

$$g^{(1)}(t) = A_1 \exp[-(t/\tau_1)^{\beta_1}] + A_2 \exp[-(t/\tau_2)^{\beta_2}] \quad (9)$$

where the exponent $\beta$ characterizes the width of the corresponding decay. For a single-exponential process, $\beta = 1$; for relaxations generated by (short-range) density fluctuations in a homopolymer melt, a typical value might be $\beta \approx 0.35$. Figure 9 shows $\beta$ values obtained for the cluster mode and the heterogeneity mode on the sample PVCH−PEE, as a function of temperature. The cluster mode has $\beta \approx 1$ throughout the temperature range investigated, spanning 40 °C above and 30 °C below the ODT. On the other hand, for the heterogeneity mode $\beta \approx 0.8$ at high temperatures, indicating that the process is slightly broader than a single exponential, and then ∼20 °C above ODT $\beta$ decreases, reaching a value of ∼0.55 at the lowest temperature examined. One might be tempted to attribute this observation to a separation of diffusivities parallel and perpendicular to the lamellar planes, in transient ordered regions appearing in the homogeneous phase, with the anisotropy becoming more pronounced as $T_{ODT}$ is crossed.[17,40] This, however, is not the case; such an effect would produce a broadening on the slower side of the heterogeneity mode, whereas we demonstrate below that it is exactly the opposite which occurs. Note that the weak internal mode contribution is inconsequential in this kind of data treatment.

Standard REPES analysis of the subtracted correlation functions for PVCH−PEE indicated that at low temperatures the heterogeneity mode splits into two components. Therefore the subtracted correlation functions at all temperatures were reanalyzed, varying the regularization strength down to a value of probability to reject PR = 0.1−0.01. The resulting spectra of decay times are presented in Figure 10, for the various temperatures indicated. It is clear that the broadening of the heterogeneity mode with decreasing temperature actually reflects the presence of two distinct dynamic processes, which have different temperature dependences for their relaxation times. At temperatures above 250 °C the two decay times are within a factor of 3, so that they cannot be separated by Laplace inversion even with lowering the regularization strength. However, the persistence of the two processes at temperatures above 250 °C is evident through the value of the $\beta$ parameter as shown in Figure 9.

The correlation functions were reanalyzed in a similar way for PEP−PEE-2, which is particularly important because values of $D_s$ are known (see Figure 7). Figure 11 shows the distribution of decay times for this sample at 180 °C, calculated with PR = 0.01. The arrows indicate the relaxation times corresponding to the internal mode, calculated from rheological data (see Figure 8), and to $D_s$ obtained by FRS. A third component, with relaxation time 1 order of magnitude less than that of self-diffusion, is observed in the distribution of decay times, as was the case in Figure 10 for PVCH−PEE. This intermediate component also appears in Figure 6 in the diffusion grid, with its maximum located at the same place, log $\tau \approx 3.3$.

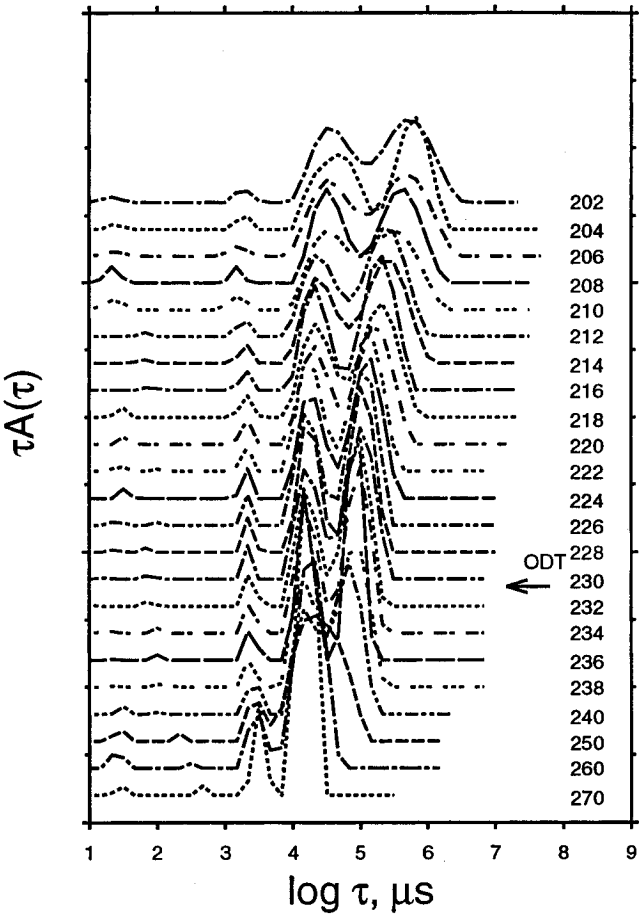


**Figure 10.** Distribution of decay times at the indicated temperatures and $\theta = 90$ °C, for PVCH−PEE-2, using a smaller regularization strength PR = 0.01−0.1.

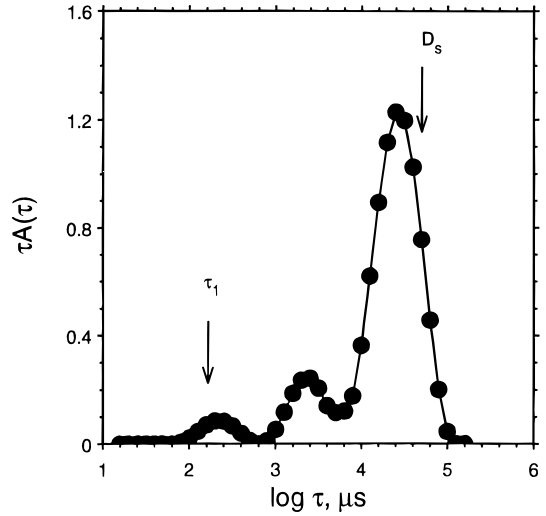


**Figure 11.** Distribution of decay times for PEP−PEE-2 at $\theta$ = 90° and 180 °C, after subtraction of the cluster mode, with PR = 0.01.

The results for PEP−PEE-2 are summarized, as a function of temperature, in Figure 12. The internal mode is plotted as $\Gamma_I/q^2$, so that it corresponds to the vertical axis ($D$ in cm$^2$/s). The original 5-fold mismatch between $D_H$ and $D_s$ in Figure 7 has diminished, and $D_H$ now corresponds more closely to $D_s$. The diffusion coefficient of the new intermediate mode, $D_x$, is also plotted in Figure 12. Its temperature dependence parallels that of $\tau_1$ and $D_H$ at high temperatures, but closer to $T_{ODT}$, the dependence is weaker than for $D_H$,

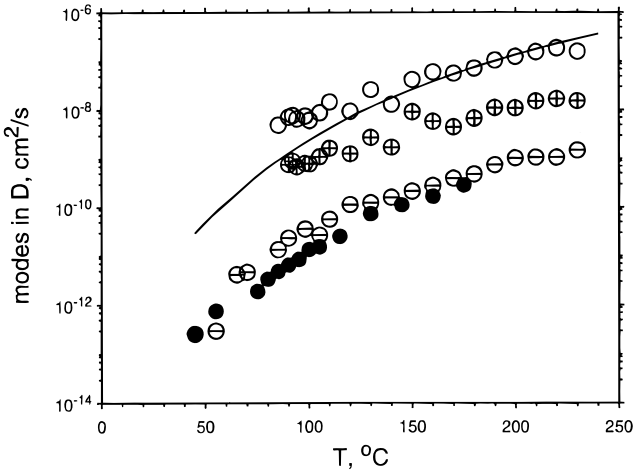


**Figure 12.** Temperature dependence of the various dynamic modes for PEP−PEE-2: (●) self-diffusion from FRS; (⊖) heterogeneity diffusion mode $D_H$; (⊕) intermediate diffusion mode $D_x$; (○) internal mode as $\Gamma_I/q^2$ ($\theta = 90°$). The full line represents the rheological longest relaxation time, as in Figure 7.

analogous to what is observed in Figure 10 for PVCH−PEE. The physical origins of this mode are not clear and are the subject of continuing investigation. The dynamics are clearly intermediate between relaxation of a single chain and translational diffusion, which could implicate the fluctuations that are visible rheologically in the same time window. For example, for PEP−PEE-2, $G'$ exhibits a failure of time−temperature superposition at a frequency designated $\omega_c$.[10] For $\omega \leq \omega_c$, a shoulder appears on the $G'$ curve, which has been attributed to the relaxation of concentration fluctuations. The time $\tau_c = 1/\omega_c$ lies between $\tau_1$ and $\tau_D$, where $\tau_D$ is defined as $1/D(q^*)^2$, where $q^*$ is the location of the peak of the structure factor. Thus, the intermediate mode could reflect the relaxation of concentration fluctuations that are weakly visible in the DLS experiment for the same reason that the heterogeneity mode appears. Recalling that resolution of this mode results in more quantitative agreement between the values of $D_s$ and $D_H$ undercuts the speculation that this mode appears merely as a result of the data treatment.

## Summary

Dynamic light scattering measurements have been performed on four block copolymer melts as a function of temperature; in all cases results were obtained above and below the ODT. Four distinct modes were resolved, with the following characteristics:

(i) The cluster mode is the dominant mode for all four samples. It corresponds to a diffusive process and contributes a single exponential to the correlation functions. Above the ODT, the associated cluster size is independent of temperature and of order 100 nm. For two samples (PEP−PEE and PVCH−PEE), this apparent size remains unchanged below the ODT, whereas for the other two samples (PE−PEE and PVCH−PE) it increases by 2 orders of magnitude at the ODT. For PEP−PEE, angle-dependent static light scattering also indicated a temperature-independent correlation length of 100 nm.

(ii) The heterogeneity mode, corresponding to translational diffusion of the chains, was resolved for all four samples, and for PEP−PEE, it was shown to be in good agreement with self-diffusion measurements by forced Rayleigh scattering.

(iii) The internal mode, a low-amplitude, $q$-independent relaxation process, was resolved, and for PEP−PEE, the associated time constant was in quantitative agreement with the longest viscoelastic relaxation time in the disordered state.

(iv) A fourth, very weak diffusive mode was resolved for PEP−PEE and PVCH−PEE; it was intermediate in time scale between translational diffusion and the internal mode relaxation time. Its origin is unclear but may reflect the relaxation of concentration fluctuations.

**Acknowledgment.** We acknowledge support from the National Science Foundation through the Grants DMR-9018807 (T.P.L.) and CHE-9203173 (a U.S.−Czech Cooperative Research award from the Division of International Programs), Grant 203/94/0817 of the Grant Agency of the Czech Republic, and from the Center for Interfacial Engineering, an NSF-sponsored Engineering Research Center at the University of Minnesota.

## References and Notes

(1) See, for example: Bates, F. S.; Fredrickson, G. H. *Annu. Rev. Phys. Chem.* **1990**, *41*, 525, and references therein.
(2) Leibler, L. *Macromolecules* **1980**, *13*, 1602.
(3) Barrat, J.-L.; Fredrickson, G. H. *J. Chem. Phys.* **1991**, *95*, 1281.
(4) Olvera de la Cruz, M. *Phys. Rev. Lett.* **1991**, *67*, 85.
(5) Fredrickson, G. H.; Helfand, E. *J. Chem. Phys.* **1987**, *87*, 697.
(6) Bates, F. S.; Rosedale, J. H.; Fredrickson, G. H. *J. Chem. Phys.* **1990**, *92*, 6255.
(7) Rosedale, J. H.; Bates, F. S.; Almdal, K.; Mortensen, K.; Wignall, G. D. *Macromolecules* **1995**, *28*, 1429.
(8) Förster, S.; Khandpur, A. K.; Zhao, J.; Bates, F. S.; Hamley, I. W.; Ryan, A. J.; Bras, W. *Macromolecules* **1994**, *27*, 6922.
(9) Hajduk, D. A.; Harper, P. E.; Gruner, S. M.; Honeker, C. C.; Kim, G.; Thomas, E. L.; Fetters, L. J. *Macromolecules* **1994**, *27*, 4063.
(10) Rosedale, J. H.; Bates, F. S. *Macromolecules* **1990**, *23*, 2329.
(11) Stepanek, P.; Lodge, T. P.; Bates, F. S. *Polym. Prepr. (Am. Chem. Soc., Div. Polym. Chem.)* **1994**, *35* (1), 616.
(12) Vogt, S.; Jian, T.; Anastasiadis, S. H.; Fytas, G.; Fischer, E. W. *Macromolecules* **1993**, *26*, 3357.
(13) Vogt, S.; Anastasiadis, S. H.; Fytas, G.; Fischer, E. W. *Macromolecules* **1994**, *27*, 4335.
(14) Jian, T.; Anastasiadis, S. H.; Fytas, G.; Adachi, K.; Kotaka, T. *Macromolecules* **1993**, *26*, 4706.
(15) Stepanek, P.; Lodge, T. P. In *Light Scattering: Principles and Development*; Brown, W., Ed.; Oxford University Press: New York, 1995.
(16) Dalvi, M. C.; Eastman, C. E.; Lodge, T. P. *Phys. Rev. Lett.* **1993**, *71*, 2591.
(17) Dalvi, M. C.; Lodge, T. P. *Macromolecules* **1994**, *27*, 3487.
(18) Kanaya, T.; Patkowski, A.; Fischer, E. W.; Seils, J.; Glaser, H.; Kaji, K. *Acta Polym.* **1994**, *45*, 137.
(19) Benmouna, M.; Duval, M.; Borsali, R. *J. Polym. Sci., Polym. Phys. Ed.* **1987**, *25*, 1839.
(20) Benmouna, M.; Benoit, H.; Borsali, R.; Duval, M. *Macromolecules* **1987**, *20*, 2620.
(21) Akcasu, A. Z.; Hammouda, B.; Lodge, T. P.; Han, C. C. *Macromolecules* **1984**, *17*, 759.
(22) Akcasu, A. Z.; Benmouna, M.; Benoit, H. *Polymer* **1986**, *27*, 1935.
(23) Semenov, A. N.; Fytas, G.; Anastasiadis, S. H. *Polym. Prepr. (Am. Chem. Soc., Div. Polym. Chem.)* **1994**, *35* (1), 618.
(24) Jian, T.; Anastasiadis, S. H.; Semenov, A. N.; Fytas, G.; Adachi, K.; Kotaka, T. *Macromolecules* **1994**, *27*, 4762.
(25) Jian, T.; Anastasiadis, S. H.; Semenov, A. N.; Fytas, G.; Fleischer, G.; Vilesov, A. D. *Macromolecules* **1995**, *28*, 2439.
(26) Pusey, P. N.; Fijnaut, H. M.; Vrij, A. *J. Chem. Phys.* **1982**, *77*, 4270.
(27) Liu, Z.; Pan, C.; Stepanek, P.; Lodge, T. P. *Macromolecules* **1995**, *28*, 3221.
(28) Pan, C.; Maurer, W.; Liu, Z.; Lodge, T. P.; Stepanek, P.; von Meerwall, E. D.; Watanabe, H. *Macromolecules* **1995**, *28*, 1643.
(29) Larson, R. G.; Fredrickson, G. H. *Macromolecules* **1987**, *20*, 1897.
(30) Gehlsen, M. D.; Bates, F. S. *Macromolecules* **1994**, *27*, 3611.
(31) Bates, F. S.; Rosedale, J. H.; Bair, H. E.; Russell, T. P. *Macromolecules* **1989**, *22*, 2557.
(32) Stepanek, P. In *Dynamic Light Scattering: the Method and Some Applications*; Brown, W., Ed.; Oxford University Press: New York, 1993.
(33) Jakes, J. *Czech. J. Phys.* **1988**, *38*, 1305.
(34) Jakes, J. *Collect. Czech. Chem. Commun.* **1995**, *60*, 1781.
(35) Provencher, S. W. *Comput. Phys. Commun.* **1982**, *27*, 229.
(36) Stepanek, P.; Lodge, T. P., unpublished results.
(37) Provencher, S. W. In *Laser Light Scattering in Biochemistry*; Harding, S. E., Sattelle, D. B., Bloomfield, V. A. Eds.; Royal Society of Chemistry: London, 1992.
(38) Stepanek, P.; Johnsen, R. M. *Collect. Czech. Chem. Commun.* **1995**, *60*, 1941.
(39) Stepanek, P.; Provencher, S. W. In *PARTEC 95, International Conference on Particle Technology*; Nurnberg, 1995; p 193.
(40) Dalvi, M. C.; Lodge, T. P. *Macromolecules* **1993**, *26*, 859.

MA9509772